

98-342



СООБЩЕНИЯ
ОБЪЕДИНЕННОГО
ИНСТИТУТА
ЯДЕРНЫХ
ИССЛЕДОВАНИЙ

Дубна

98-342

E1-98-342

G.Borchert¹, A.K.Kacharava², V.I.Komarov, A.V.Kulikov,
M.S.Nioradze³, G.G.Macharashvili², H.Müller⁴,
A.Yu.Petrus, S.V.Yaschenko

FEASIBILITY TO STUDY THE INCLUSIVE
PRODUCTION OF FAST NUCLEAR FRAGMENTS
AT THE ANKE SPECTROMETER

¹IKP, FZ-Jülich, Germany
²Permanent address: HEPI TSU, Tbilisi, Georgia
³HEPI TSU, Tbilisi, Georgia
⁴IKPH, FZ-Rossendorf, Dresden, Germany

1998

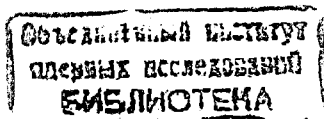
Introduction

One of the basic types of interactions of fast projectiles with nuclei consists of processes with few-nucleon groups involved. Then the projectile-nucleus interaction proceeds with some probability as quasielastic scattering, resulting in the knock-out of light fragments, mainly at large angles to the beam and rather low kinetic energies. However, a significant energy is deposited into a group. When this energy exceeds about two-three hundred MeV, sufficient for excitation of nucleon internal degrees of freedom, the process acquires a distinctly cooperative behavior. The deposited energy becomes dispersed between the participating nucleons of the target nucleus and a phenomenological concept of "excitation" or "heating" of the few-nucleon systems is relevant. It is essential that such an excited piece of nuclear matter receives inevitably some velocity in the target-nucleus rest frame corresponding to a momentum resulting from the energy-momentum conservation.

There are different ways of deexcitation for such a moving excited few-nucleon group. The excitation energy can concentrate as the kinetic energy of one of the nucleons. Therefore, the nucleon can be emitted far beyond the boundary of the kinematical region available for the interaction of the projectile with a single target nucleon being at rest (or moving with a normal Fermi-momentum). Such a process is well-known as cumulative particle emission. The excitation energy can also convert into the invariant mass and kinetic energy of produced particles. If this energy exceeds the energy initially available in the projectile-rest-nucleon system, one deals with so-called subthreshold production. These two phenomena have already been observed for many years and are under intensive study in a great number of experiments.

Extensive data on cumulative processes have revealed very prominent features. In particular, the above mentioned velocity of the excited group results in a pronounced angular anisotropy of the cumulative particle emission, seen in experiments. Another significant feature of cumulative spectra is their independence of the initial energy and the type of the projectile particles. It may be considered as a clear evidence for the fact that such cumulative processes exhibit just the properties of the locally high-excited nuclear matter and do only weakly depend on the way of its excitation. Unfortunately, practically all available data suffer from the same disadvantage: they were obtained in inclusive experiments, mostly with only single-particle differential cross sections measured. Exceptionally, double-particle differential cross-sections have been investigated, but the number of measured kinematical observables was insufficient for a strict reconstruction of the interaction events. The mechanism of the process cannot be studied unambiguously in such inclusive experiments. For the processes under discussion the existing experimental data do not give the answer to the questions of importance:

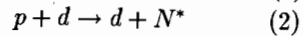
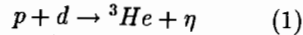
- how many nucleons participate in the process ?



- what amount of energy is deposited into the few-nucleon group ?
- is the participating nucleon group in the initial state of the target-nucleus a correlated system or only a set of noncorrelated separate nucleons exposed to some subsequent interactions during the process?

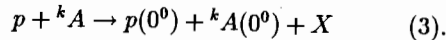
Therefore, the cumulative and subthreshold production data are still at a stage of very tentative interpretation. In particular, a question of fundamental character stays with no answer: are such phenomena an evidence for a specific hadronic state of the heated nuclear matter, or are they a manifestation of some characteristic elementary subprocesses (such as $NN, N\Delta, NN^*, \pi N$ -scattering) specific for few-nucleon systems at high energies.

In this situation two main streams of investigation can be seen. One is a detailed, exclusive study of the cooperative processes in their simplest forms. COSY20 proposal "Exclusive deuteron break-up study with polarized protons and deuterons at COSY" [1] approved for the spectrometer ANKE is just a study of this type. The detailed analysis of mechanism of the processes



suggested in ref. ([2] - [5]) is another study in this stream appropriate for ANKE.

The other approach is a search of new experimental manifestations of interactions of projectile particles with few-nucleon groups at high energy-momentum transfers. One of such manifestations may reveal in a special situation when the excitation energy "absorbed" by the nucleon group is totally consumed by meson production. Then there is no energy left for the relative motion of free unbound nucleons. The nucleon group, cooled in this way, can stick together, coalesce to a bound state as a light nucleus. The velocity, predominantly in the forward direction, gained by the group during its excitation conserves on the average as the velocity of the final light nucleus emitted at small forward angles. Thus, the process results in the production of fast forward emitted light nuclear fragments. The term "fast" means here that the fragment momentum range of interest is higher than the usual momenta of evaporated or spectator fragments. Experimental data for the production of fragments with momenta higher than 1 GeV/c at small angle, produced at light target-nuclei are very limited, even for inclusive processes, and are completely absent for double-particle differential cross-sections of the processes:



If the incidence energy is under the threshold of the proton-antiproton pair production, then the baryon number conservation limits the non-detected particles X in (3) to mesons (one or several). Thus, one gets in the process (3) a meson production in the system of k nucleons [6]. (One should stress that the process under discussion

here is quite different in its mechanism and expected characteristics from the process of diffraction dissociation of a proton on a nucleus kA producing the same final particles.)

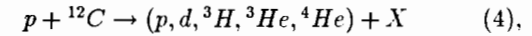
The advantage of the process (3) is that, by the measurement of the proton and the fragment momenta, one immediately gets:

- the number (k) of participating nucleons,
- the value of the energy transferred to the k -nucleon group at the initial stage of the process,
- the invariant mass and the total momentum of the meson group produced at the deexcitation stage.

Thus, the method should provide data which are more informative than those of previous studies of cumulative and subthreshold processes.

An experimental study of the above processes (1) - (3) essentially requires measurements of the momentum of fast light nuclei at small forward angles. The aim of this work is a consideration of the ANKE performance and operating conditions expected for the detection of such particles. We constrain the considerations here to characteristics of the counter part of the detector system excluding the track detection part (multiwire chambers). Such kind of information is required for tuning the trigger system for track detectors. The possibility to get information for understanding of mechanisms of fast nuclear fragment emission already at the commissioning stage of the facility is also considered.

All the characteristics are discussed here for the specific case of the process



at the incidence energy of $T_p = 800$ MeV.

It is noteworthy that the study of reaction (4) can be carried out already during the commissioning of the whole setup, its calibrations and the first measurements considered in the proposal EXP. COSY-38 [7].

Spectrometer ANKE

The spectrometer ANKE is installed at the internal beam of the proton synchrotron COSY (Institut für Kernphysik, Forschungszentrum Jülich) and is in its commissioning stage. The experiments are starting in 1998. The general layout of the ANKE facility is shown in **Fig. 1**. The main part of the setup is a triplet of dipole magnets (D1, D2 and D3). They are arranged in such a way that a steady orbit of the COSY beam passes the gaps of all the magnets resulting in a bump compared to the unperturbed orbit. (The angle of bending the beam in the D1 is denoted here as α). A target station (T) is placed between the first and the second dipole. Targets of two different types will be used in the experiments: carbon and polyethylene foils and in a late stage (hydrogen) cluster beam. The second dipole is used as the analyzing magnet for particles emitted from the target at small forward

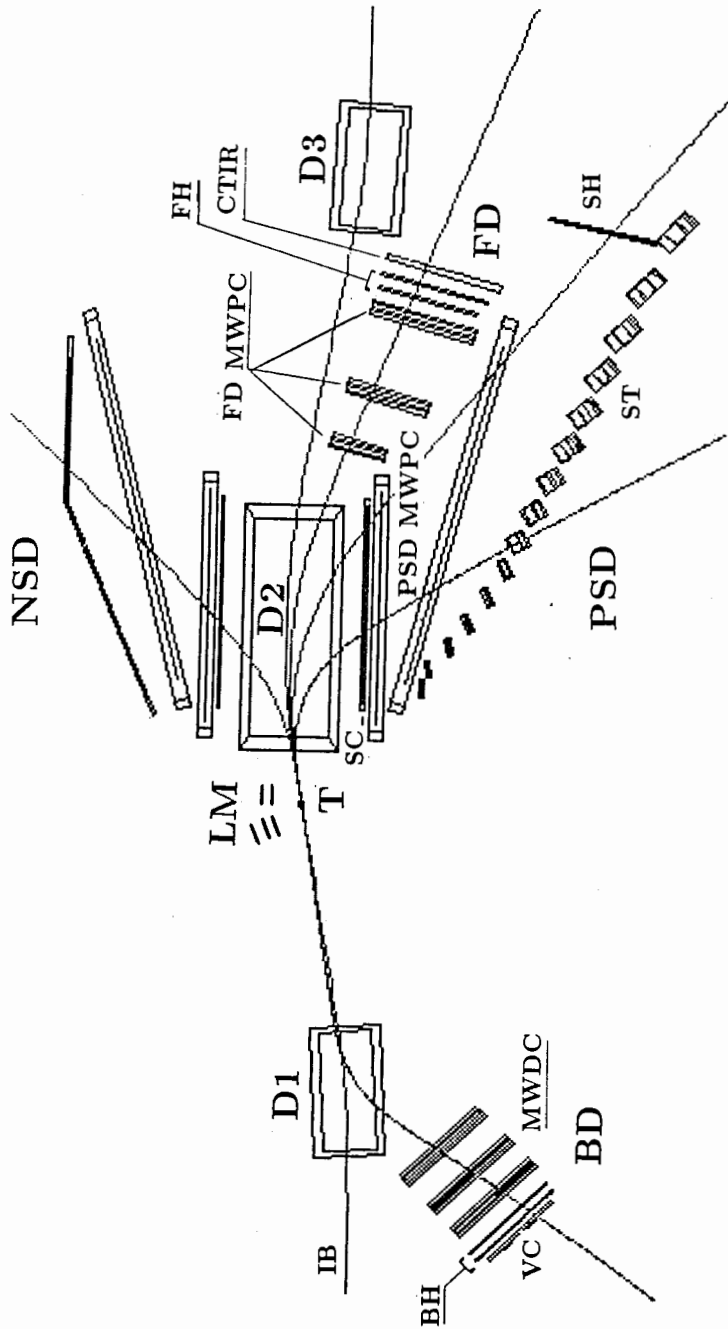


Fig.1. Layout of the ANKE facility at COSY.

angles (polar angles in the horizontal plane in the range $0 - 10^\circ$). Detector systems of the spectrometer are: Positive Side Detector (PSD) for measurements in the momentum range P/P_0 of about 0.2 - 0.6 of the primary beam momentum P_0 , Forward Detector (FD) for a P/P_0 of about 0.4 - 1.0 and Backward Detector (BD) for detection of particles emitted backwards (polar angles in the horizontal plane in range of $170^\circ - 180^\circ$). FD, PSD and BD systems provide identification of the particle type (π^+ , p , d , 3H , 3He , 4He). The identification parameters are: the bending in magnet field, the time-of-flight, energy loss, range and the Cherenkov light emission. For this aim the multiwire proportional and drift-chambers, hodoscopes of scintillation counters and of Cherenkov counters of total internal reflection are used [8].

Overview of the scintillation hodoscopes

The Backward Detector hodoscope (BH) consists of two sensitive planes, each of 8 elements (6.2 cm width, 28 cm length). The scintillators are viewed from both ends by PM's XP2020. Time and amplitude of the signals will be measured. The following characteristics have been obtained in the hodoscope test with cosmic rays [9]: the standard deviation of the time signal from one element is of 150 ps, the amplitude resolution for the 2 cm thick scintillators is 28 % (FWHM) and for 0.5 cm scintillators - 33 % (FWHM), in average. The coordinate accuracy along the element determined by the time difference of the signals from both ends of the scintillators is about 2.0 cm (RMS).

The Forward Detector Hodoscope (FH) consists of two planes of vertically oriented scintillation counters of 36 cm height. The first plane (FH1) contains 8 elements, with width and thickness of $8 \times 2 \text{ cm}^2$ for 6 elements and $4 \times 1.5 \text{ cm}^2$ and $6 \times 1.5 \text{ cm}^2$ for the ones close to the beam pipe. The second plane (FH2) contains 9 elements in total, with the corresponding dimensions of $8 \times 2 \text{ cm}^2$ for 6 counters and by one of $4 \times 1.5 \text{ cm}^2$, $5 \times 1.5 \text{ cm}^2$ and $6 \times 1.5 \text{ cm}^2$. The tests with cosmic rays [10] resulted in: the amplitude resolution for one plane is 27 % (FWHM) with nonhomogeneity of light collection (along the scintillator length) less than 8 %; the time resolution is 100-150 ps (RMS) providing the coordinate resolution of 1.5 - 2.3 cm.

The Side hodoscope (SH) consists of two sensitive planes. Each plane contain of 6 elements with a width of 10 cm and a thickness of 1 cm. We consider here in simulations only one plane of the hodoscope.

Angular-momentum acceptance of the hodoscopes

The geometrical acceptance of the FH and SH for the incident energy $T_p = 800 \text{ MeV}$ and the $\alpha=10.6^\circ$ is shown in Fig. 2(a,b). It has been obtained with ejectiles uniformly distributed in the momentum range $P_{eject} = 0 \div 2000 \text{ MeV}/c$ and emission angles $\vartheta \leq 20^\circ$. Particles were considered as detected if they passed all the detector systems and reached the second plane of the FH or the first counter plane of SH, respectively. All secondary processes, like decay in flight, multiple Coulomb scattering and hadronic interactions, were switched off in this simulation. It is seen

Table 1. Mean momentum (MeV/c) and angle (degree) with their RMS, and $\Delta p/p$ of the particles ($Z=1$) passed through the Start and Side hodoscopes (ST is a module number of the Start hodoscope and SH of the Side hodoscope).

SH/ST	#1	#2	#3	#4	#5	#6
#12	496.6 ± 11.5					
$\theta \pm \Delta\theta$	-10.71 ± .71					
$\Delta p/p$	2.3%					
#13	493.9 ± 11.5	537.5 ± 13.8				
$\theta \pm \Delta\theta$	-8.84 ± .71	-10.40 ± .73				
$\Delta p/p$	2.33%	2.57%				
#14	491.8 ± 10.9	531.4 ± 12.9	581.7 ± 17.3			
$\theta \pm \Delta\theta$	-7.05 ± .70	-8.58 ± .72	-10.23 ± .73			
$\Delta p/p$	2.21%	2.42%	2.98%			
#15	489.8 ± 10.2	526.5 ± 13.0	573.3 ± 15.1	633.9 ± 20.1		
$\theta \pm \Delta\theta$	-5.33 ± .72	-6.82 ± .73	-8.49 ± .68	-10.22 ± .69		
$\Delta p/p$	2.09%	2.47%	2.64%	3.17%		
#16	487.1 ± 9.4	523.6 ± 11.7	568.7 ± 14.4	625.4 ± 18.6	696.5 ± 24.8	
$\theta \pm \Delta\theta$	-3.54 ± .66	-5.13 ± .69	-6.89 ± .72	-8.64 ± .72	-10.42 ± .68	
$\Delta p/p$	1.93%	2.24%	2.53%	2.97%	3.56%	
#17	486.1 ± 9.0	520.8 ± 10.8	562.6 ± 13.2	614.5 ± 17.7	685.4 ± 23.3	776.8 ± 32.6
$\theta \pm \Delta\theta$	-1.87 ± .67	-3.53 ± .69	-5.22 ± .71	-6.99 ± .72	-8.89 ± .73	-10.86 ± .74
$\Delta p/p$	1.85%	2.08%	2.35%	2.88%	3.40%	4.20%
#18	485.8 ± 8.2	517.6 ± 10.2	557.8 ± 12.8	607.1 ± 15.9	672.1 ± 21.1	758.2 ± 29.9
$\theta \pm \Delta\theta$	-.30 ± .60	-1.90 ± .66	-3.63 ± .70	-5.43 ± .69	-7.36 ± .69	-9.37 ± .74
$\Delta p/p$	1.69%	1.97%	2.30%	2.62%	3.13%	3.94%
#19	487.6 ± 8.1	515.5 ± 9.6	552.6 ± 12.1	599.9 ± 15.1	661.4 ± 20.2	739.5 ± 26.6
$\theta \pm \Delta\theta$	1.02 ± .70	-.32 ± .61	-1.99 ± .67	-3.88 ± .71	-5.81 ± .74	-7.84 ± .76
$\Delta p/p$	1.66%	1.87%	2.19%	2.52%	3.05%	3.59%
#20	485.3 ± 8.2	516.9 ± 9.4	547.8 ± 11.0	593.2 ± 14.7	649.0 ± 19.0	723.0 ± 25.8
$\theta \pm \Delta\theta$	2.76 ± .70	.93 ± .71	-.41 ± .63	-2.28 ± .71	-4.24 ± .74	-6.29 ± .78
$\Delta p/p$	1.69%	1.82%	2.00%	2.47%	2.93%	3.57%
#21	483.2 ± 7.2	512.9 ± 9.2	548.2 ± 10.8	583.8 ± 13.3	639.4 ± 17.8	708.8 ± 24.0
$\theta \pm \Delta\theta$	4.48 ± .65	2.64 ± .68	.78 ± .70	-.63 ± .67	-2.72 ± .76	-4.80 ± .77
$\Delta p/p$	1.49%	1.79%	1.97%	2.28%	2.79%	3.38%
#22	480.4 ± 7.3	507.8 ± 9.0	541.7 ± 11.2	583.5 ± 12.4	624.0 ± 17.2	693.9 ± 22.4
$\theta \pm \Delta\theta$	6.21 ± .75	4.44 ± .71	2.53 ± .75	.50 ± .66	-.93 ± .77	3.25 ± .77
$\Delta p/p$	1.53%	1.77%	2.06%	2.12%	2.75%	3.23%

Momentum Acceptance of the FH and SH ($T_p=800$ MeV)

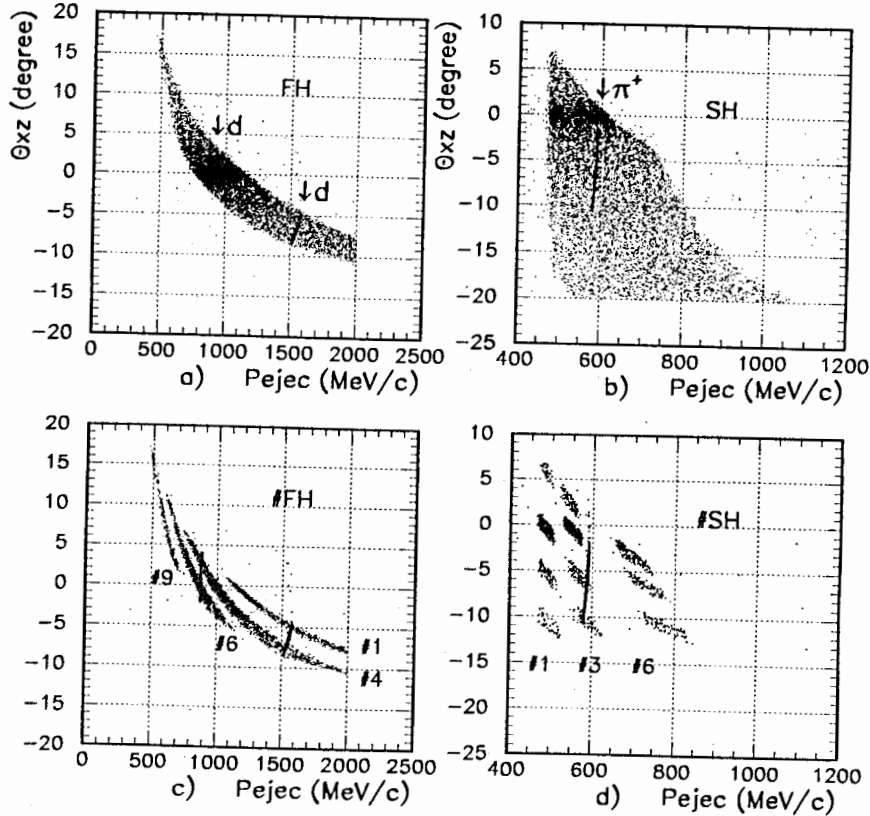


Fig.2. Angular-momentum acceptance of the Forward (a,c) and Side Hodoscopes (b,d). ϑ_{zz} - projection of the polar angle ϑ of the ejectile with momentum P_{eject} at the median-plane XZ of the spectrometer. Arrow denote the kinematical boundary for the deuteron and pion from the reaction $pp \rightarrow d\pi^+$

that the hodoscopes provide a significant momentum-angular acceptance. For small emission angles ϑ_{zz} in the median plane ($-2^\circ < \vartheta_{zz} < +2^\circ$), where the spectrometer has the maximum geometrical acceptance, the covered momentum interval is of 480 MeV/c – 620 MeV/c for the SH and 780 MeV/c – 1140 MeV/c for the FH. For the larger emission angles these intervals increase significantly:

$$\begin{aligned} &\text{for the SH } (-20^\circ < \vartheta_{zz} < +6^\circ) \text{ and } 480 \text{ MeV/c} < P_{ejec} < 1050 \text{ MeV/c}; \\ &\text{for the FH } (-10^\circ < \vartheta_{zz} < +16^\circ) \text{ and } 500 \text{ MeV/c} < P_{ejec} < 2000 \text{ MeV/c}. \end{aligned}$$

It is essential that acceptances of the two hodoscopes being complementary to each other provide measurements of the momentum and angular dependences of the double differential cross sections of the particles emission in a rather wide (p, ϑ) range.

The momentum-angle intervals given by several separate elements of the Forward hodoscope (FH: #1 – 9), and some SH modules (SH: #1 – 6) at coincidence with several Start counters (ST: #12 – 22), are shown in Fig. 2(c,d) correspondingly. These distributions have been calculated taking into account the particle interaction with the spectrometer matter. The mean values of momentum and angle for the single charged particles are listed in Table 1.

It is seen, that in the Side hodoscope together with the start counters ST provides measurement of momentum and angle of the particles emission with a rather high accuracy ($\Delta p/p \approx 1.5 - 4.0\%$; $\Delta \theta \approx 0.6 - 0.8^\circ$). For the forward hodoscope counters alone the accuracy is much worse ($\Delta p/p \approx 10 - 15\%$) since there is no start counters in the FD. Therefore, if to study the process (4) at the early stage using only information from the hodoscopes, it would be appropriate to arrange the FH immediately after the SH and to use them together. It should improve the accuracy of the momentum measurement (for higher accuracy of the coordinate measurements) and reliability of the particle type identification (for ΔE -measurements in 3 or 4 planes of the scintillation counters).

Spectra of light nuclear fragments in the framework of the ROC-model

Estimations of the expected cross sections of the fragment production and the respective counting rates of the detectors have been done using the Rossendorf Collision Model (ROC-Model). The model has been successfully used to reproduce known experimental data on cumulative and subthreshold processes ([11], [12], [13]). The model provides calculations of the differential cross sections of the process (4) as well as the inclusive cross sections of processes:

$$p + A \rightarrow (d, {}^3\text{H}, {}^3\text{He}, {}^4\text{He}) + X \quad (5).$$

In the region of small emission angles and high momenta one should expect a significant contribution of the mechanism of meson production in few-nucleon groups in nuclei (effect of "meson cooling" [6]). It should manifest itself in a production rate

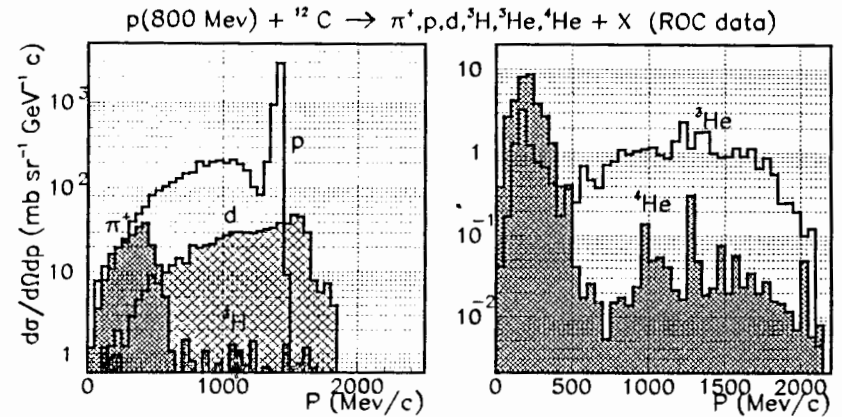


Fig.3. Momentum spectra of secondary particles ($Z=1, Z=2$) from the process (4) obtained within the ROC model.

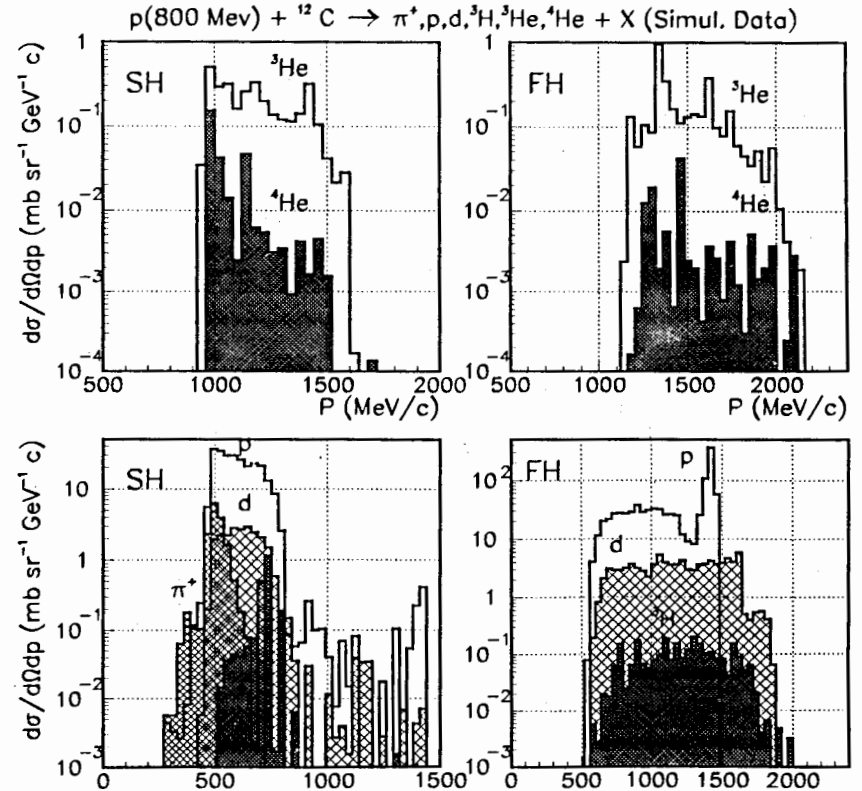


Fig.4. Momentum spectra of particles detected in the Forward and Side hodoscope from the process (4).

of high-momentum fragments significantly higher than predicted by mechanisms considering only single-nucleon interactions. However, the model requires for describing the fragment emission one special parameter, determining the probability to get a bound state (nuclear fragment) in a group of nucleons with low relative momenta. Each kind of the fragments requires its special coalescence parameter, but values of them are poorly known. So, the reliability and accuracy of the model predictions for the high-momentum parts of the spectra may be improved by fitting the intensive low-momentum parts of the spectra generated by more traditional and better investigated mechanisms, which also include the same coalescence parameters.

An advantage of the model is that it has been implemented as a standard computer code. That allows to use it in the simulations as an event-generator [8]. Then counting rates of the events in different combinations of SH and ST counters can be immediately compared with the model predictions. Such experimental factors as Coulomb scattering, nuclear interactions in the spectrometer materials and a rather complicated shape of the momentum-angle acceptances (Fig. 2.d) may be properly taken into account by this approach.

The momentum spectra of secondary particles from the process (4) generated with the ROC-Model are presented in Fig. 3. The spectra for all types of secondaries detected in the Forward- and Side hodoscopes are shown in Fig. 4. It is seen that the high-momentum part of spectra is detected in the Forward hodoscope. Nevertheless, study of the spectra in the Side hodoscope will give significant information. In particular, it should give the information for coalescence parameter values and show to what extent the model is capable to reproduce simultaneously the differential cross sections of emission of a big set of particles: π^+ , p , d , 3H , 3He , 4He .

Expected counting rates

Table 2 lists inclusive production cross sections $\sigma_i(\Delta\Omega)$ for various types of particles produced in the reaction $p + {}^{12}C \rightarrow (\pi^+, p, d, {}^3H, {}^3He, {}^4He) + X$, and detected in the Forward and Side hodoscope. The cross sections $\Delta\sigma_i$ expressed in mb are the integrals of the differential cross section over the angular-momentum acceptance with taking into account the detection probability $\varepsilon_i(\vec{p})$:

$$\Delta\sigma_i \approx \int \frac{d^3\sigma}{d\vec{p}} \varepsilon_i(\vec{p}) d\vec{p}.$$

Here the detection probability $\varepsilon_i(\vec{p})$ is determined only by the angular-momentum acceptance of the detector, but effects of particle interaction in spectrometer materials also can be introduced into calculations. The cross sections are given separately for each particle produced in (4).

Table 2. Inclusive integrated cross sections (mb) for particles from the reaction $p(800) + {}^{12}C \rightarrow \pi^+, p, d, {}^3H, {}^3He, {}^4He + X$ detected in the Forward and Side hodoscopes.

particle(<i>i</i>)	π^+	p	d	3H	3He	4He
$\sigma_i(\Delta\Omega)mb$	1.065	34.350	3.330	0.126	0.180	0.1700
$\Delta\sigma_i(mb)$ FH	0.001	3.780	0.350	0.010	0.013	0.0004
$\Delta\sigma_i(mb)$ SH	0.045	0.720	0.063	0.005	0.012	0.0010

The expected counting rates n_i can be found multiplying the cross sections $\Delta\sigma_i$ by the beam-target luminosity L . At the luminosity $L = 1.0 \cdot 10^{31} \text{ cm}^{-2} \text{ s}^{-1}$, the total counting rate for the various particles in the Side hodoscope is equal to :

$$\begin{aligned} n_p &= 0.720 \text{ mb} \cdot L \approx 7.0 \cdot 10^3 \text{ s}^{-1}, \\ n_d &= 0.063 \text{ mb} \cdot L \approx 6.0 \cdot 10^2 \text{ s}^{-1}, \\ n_{\pi^+} &= 0.045 \text{ mb} \cdot L \approx 5.0 \cdot 10^2 \text{ s}^{-1}, \\ n_{{}^3He} &= 0.012 \text{ mb} \cdot L \approx 1.2 \cdot 10^2 \text{ s}^{-1}, \\ n_{{}^3H} &= 0.005 \text{ mb} \cdot L \approx 5.0 \cdot 10^1 \text{ s}^{-1}, \\ n_{{}^4He} &= 0.001 \text{ mb} \cdot L \approx 1.0 \cdot 10^1 \text{ s}^{-1}. \end{aligned}$$

The obtained values show that the processes under consideration can be measured with a good statistical accuracy during a reasonable beam-time at ANKE.

Particle identification

Let us examine the possibility to separate with the Side hodoscope the particles (π^+ , p , d , 3H , 3He , 4He), which participate in the process (4). The ΔE and TOF spectra have been simulated to estimate the reliability of the identification and the background suppression by the Side Hodoscope elements alone. Uniformly distributed events in the interval of angles $\vartheta < 10^\circ$ were used as event generator in this simulation.

Fig. 5(a, b, c) displays the distribution of energy losses (ΔE) and time-of-flight (TOF) for the particles: (π^+ , p , d , 3H , 3He , 4He), in the Side Hodoscope elements (#1, #3, #6) with the mean momenta of 485 MeV/c, 547 MeV/c and 693 MeV/c, respectively. It is noteworthy that the use of both ΔE - and TOF- spectra allows to improve the particle identification: in some cases when one of the methods is ineffective, the other one helps to separate the particles. It is obvious that the energy loss resolution and time resolution of the whole hodoscope system can be improved when the information from four scintillator planes is used. This can be achieved if the FH is moved from its standard position in the Forward detector and placed for this particular measurements just after the SH. Such an arrangement can be especially useful for the measurement of particles with a relatively low intensity (e.g. the 3H - rate is about of 10^3 times less than the rate of protons).

Thus, one may expect quite reliable and reasonable data on the double differential cross sections of the fragment production using only scintillation hodoscopes information.

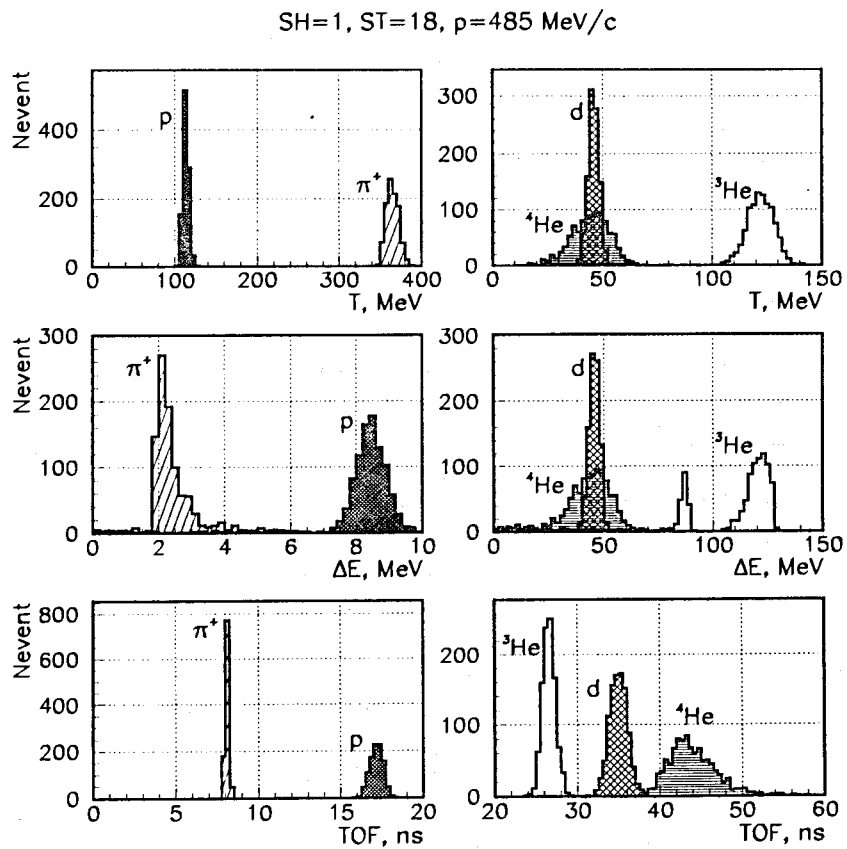


Fig.5.a. ΔE and Time of flight spectra for the Side hodoscope modules.

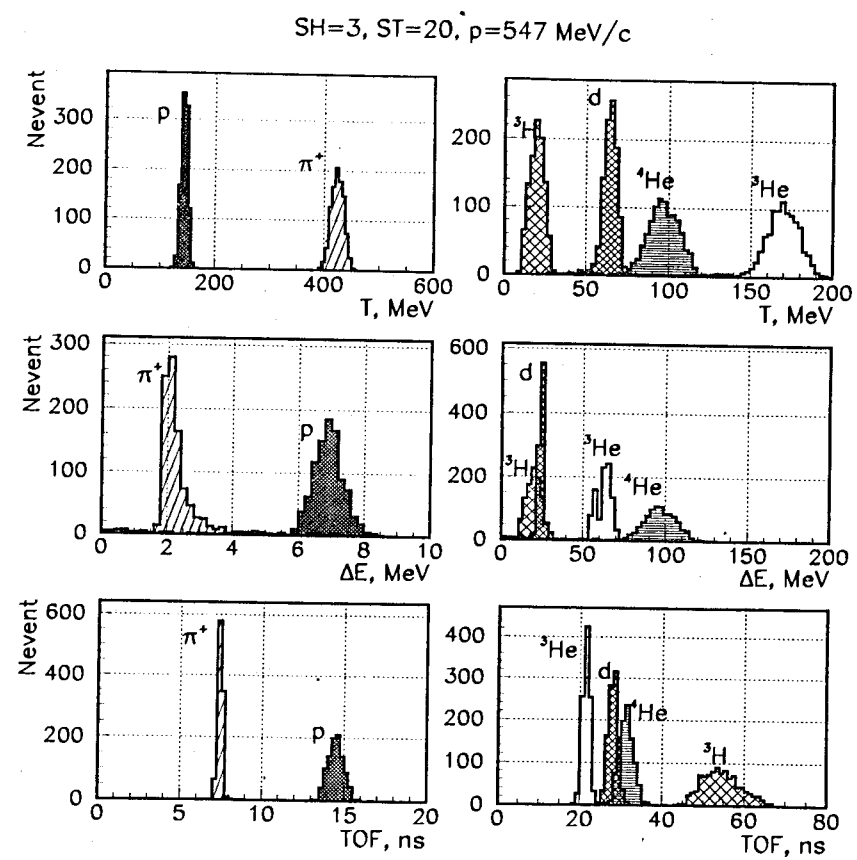


Fig.5.b. ΔE and Time of flight spectra for the Side hodoscope modules.

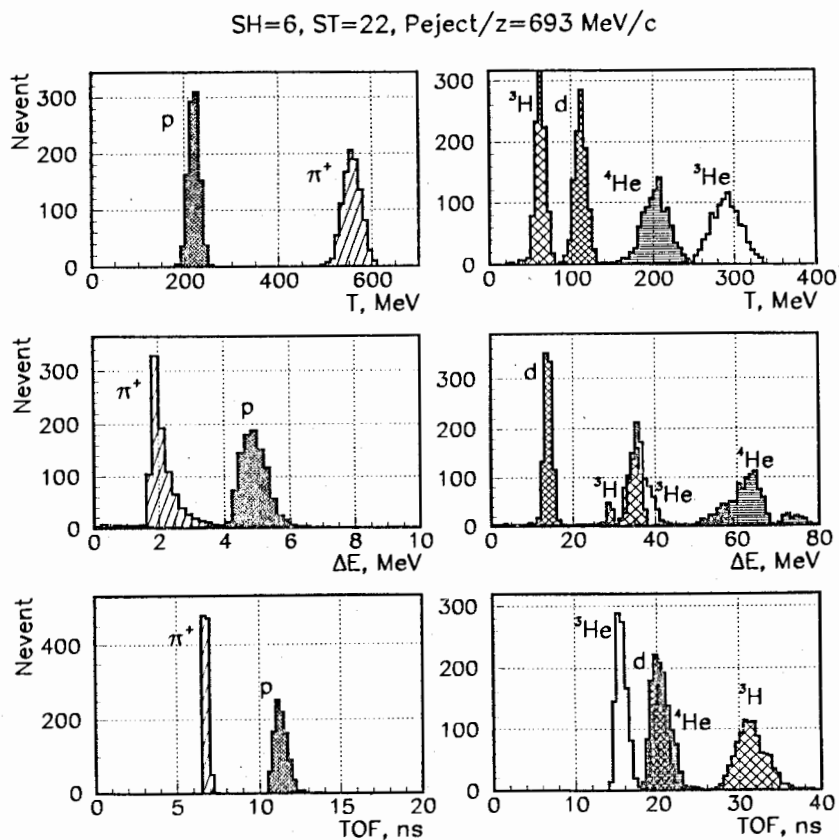


Fig.5.c. ΔE and Time of flight spectra for the Side hodoscope modules.

Conclusion

The conditions to study the inclusive spectra of fast nuclear fragments at the ANKE spectrometer have been simulated in its commissioning stage. It is shown that counter system of the setup can provide reliable identification of the processes under consideration. The simulation shows also a reasonable level of the counting rates expected in such experiments.

Acknowledgment

We are very obliged to Prof.K.Sistemich and Yu.N.Uzikov for useful discussions.

The investigation was supported by the grants RFBR No. 96-02-17215, WTZ No. RUS-667-97, INTAS-Georgia No. 98-505.

References

- [1] S.Dshemuhadse et al., COSY Proposal 20, KFA Jülich (1992).
- [2] L.A.Kondratyuk, A.Lado, Yu.Uzikov, Yadernaia Fizika, vol.58 (1995), p.524
- [3] L.A.Kondratyuk, Yu.Uzikov, JETP Letters, vol.63 (1996), p.3
- [4] L.A.Kondratyuk, Yu.Uzikov, Yadernaia Fizika, vol.60 (1997), p.1603
- [5] Yu.N.Uzikov, Yadernaia Fizika, vol.60 (1997), p.1771
- [6] V. Komarov, A. Petrus, H. Müller, Proc. of Int. Conf. on Physics with GeV-Particle Beams, World Scientific Publishing, ISBN 981-02-2279-3 (1995) 456.
- [7] V.P.Koptev et al., COSY Proposal 38, KFA Jülich (1997)
- [8] A.K.Kacharava et al., JINR report, E1-97-324, Dubna (1997)
- [9] V.Komarov et al., KFA Annual Rep. 1996 Jülich (1997) p.67
- [10] V.Komarov et al., KFA Annual Rep. 1997 Jülich (1998) p.xx
- [11] H.Müller, Z.Phys., A353, (1995), p.103; A353, (1995), p.237
- [12] H.Müller, K.Sistemich, Z.Phys., A344, (1992), p.197
- [13] A.Sibirtsev et al., Z.Phys, A351, (1995), p.333

Received by Publishing Department
on December 10, 1998.